Dual-Band Imaging of Military Targets Using a QWIP Focal Plane Array

A. Goldberg, T. Fischer and S. Kennerly
EO/IR Technology Branch, Army Research Laboratory, Adelphi, MD 20783
and
S. Wang, M. Sundaram, P. Uppal, and M. Winn
Advanced Technology Division, Sanders, A Lockheed Martin Company
Nashua, NH 03060
and
G. Milne and M. Stevens
Lockheed-Martin Electronics and Missiles
Orlando, FL 32819

Abstract

We present dual-band infrared image data collected as part of the Multidomain Smart Sensors effort at the U. S. Army Research Laboratory (ARL). The goal of this effort is to produce large-format, staring focal plane arrays (FPAs) that are able to see the battlefield in both the 3 to 5-μm (mid-wave infrared or MWIR) and 8 to 12-μm (long-wave infrared or LWIR) atmospheric transmission windows. The data was collected under laboratory and field test conditions using a simultaneously integrating, pixel-registered, 256 x 256, dual-band focal plane array produced by Lockheed Martin using quantum-well infrared photodetector (QWIP) technology. The dual-band FPA was installed in a camera that was taken in the field to gather image data on military targets. The pixel-registered dual-band FPA is well suited for the application of image fusion algorithms. We also applied some of these image fusion techniques to the imagery to enhance the visibility of targets.

1.0 INTRODUCTION

Over the last few years, much effort has been invested in producing dual-band infrared (IR) imaging. Some of the motivations behind such efforts are enhanced detection of targets in clutter, the ability to distinguish between targets and decoys, and remote absolute temperature measurement. These efforts have produced infrared focal plane arrays (FPAs) operating at two wavelengths in the mid-wave infrared[1] (MWIR, 3 to 5 μm) and FPAs operating at two wavelengths in the long-wave infrared[2] (LWIR, 8 to 12 μm) and also FPAs operating in both the LWIR and MWIR[3] spectral regions. In earlier efforts, the pixels of the individual colors were either not spatially registered or the outputs were read out sequentially (not simultaneously).

---

[1] J. Caufield, *et al*, "Simultaneous Integrating Staring Two Color IRFPAs," *Proceedings of the 1997 IRIS Detector Specialty Group Meeting on Detectors,* p. 351, ERIM (1998).
[2] M. Sundaram, *et al*, "Advances in QWIP FPA (2-Color and 1-Color) Technology," *Proceedings of the 1998 IRIS Specialty Group Meeting on Detectors*, p. 219, ERIM (1999).
[3] D. Scribner, J. Schuler, P. Warren, M. Satyshur, M. Kruer, "Infrared Color Vision: Separating Objects from Backgrounds," *Proceedings of the SPIE - Infrared Detectors and Focal Plane Arrays V*, Vol. 3379, p. 2 (1998).

Report Documentation Page

Report Date	Report Type	Dates Covered (from... to)
00012001	N/A	-

Title and Subtitle Dual-Band Imaging of Military Targets Using a QWIP Focal Plane Array	**Contract Number**
	Grant Number
	Program Element Number
Author(s) Goldberg, A.; Fischer, T.; Kennerly, S.; Wang. S.; sundaram, M.; Uppal, P.; Winn, M.; Milne, G.; Stevens, M.	**Project Number**
	Task Number
	Work Unit Number
Performing Organization Name(s) and Address(es) EO/IR Technology Branch, Army Research Laboratory Adelphi, MD 20783	**Performing Organization Report Number**
Sponsoring/Monitoring Agency Name(s) and Address(es) Director, CECOM RDEC Night Vision and Electronic Sensors Directorate, Security Team 10221 Burbeck Road Ft. Belvoir, VA 22060-5806	**Sponsor/Monitor's Acronym(s)**
	Sponsor/Monitor's Report Number(s)
Distribution/Availability Statement Approved for public release, distribution unlimited	
Supplementary Notes The original document contains color images.	
Abstract	
Subject Terms	
Report Classification unclassified	**Classification of this page** unclassified
Classification of Abstract unclassified	**Limitation of Abstract** UNLIMITED
Number of Pages 20	

Recently, the Army Research Laboratory (ARL), in federation with several industry and academic partners, has developed the concept of a multi-domain smart sensor (MDSS).[4] This conceptual or "technology demonstration" system is envisioned as a single unit combining both passive and active sensor components with advanced signal processing and aided target recognition (ATR) tools. Such a sensor would enhance situational awareness on the battlefield in all ambient conditions by locating and classifying threats with increased effectiveness over existing systems. An integral part of the MDSS system is a dual-band infrared imager operating in the MWIR and LWIR bands. This imager would be advantageous over single-color IR cameras (either LWIR or MWIR) because it can operate in a wider range of ambient conditions and be more effective in defeating IR countermeasures such as smoke, camouflage, and flares. The MDSS program has supported research aimed at producing large-format, staring, dual-band FPAs. Both quantum well infrared photodetector[5] (QWIP) and mercury-cadmium telluride (HgCdTe or MCT) technologies were investigated. This paper presents the results for the QWIP devices.

The quantum well infrared photodetector is made with GaAs and other III-V semiconductors, and has been put forward as an alternative to the incumbent MCT devices for dual-band infrared FPAs. The QWIP detector structure has the advantage over an MCT detector because the spectral response is relatively narrow which means that a detector designed for the 8 to10-μm wavelength band detects light only in that band with little or no "spectral crosstalk" with a detector in the 3 to 5-μm band. QWIPs have been designed and demonstrated to operate effectively at peak wavelengths as short as 3 μm to longer than 16 μm. Dual-band detector structures present no serious materials growth issues because, for the most part, the operating wavelengths are determined by the thicknesses of the layers, a feature easily controlled with molecular beam epitaxy (MBE). In addition, the material growth and processing technology are more mature in the III-V material systems than II-VI materials like MCT, allowing for high operability of FPAs with uniform pixel-to-pixel response, which is the main performance limitation of modern IR FPAs.

The principal disadvantages of QWIPs are their low single-pixel quantum efficiency relative to MCT and relatively high dark currents at temperatures near that of liquid nitrogen (77 K). The high dark current at 77 K necessitates cooling to temperatures around 65 K or below to obtain background-limited performance (BLIP) in LWIR QWIPs. Nevertheless, excellent IR imagery has been demonstrated with large format (640×480 pixels) FPAs.

We will describe the fabrication and test results of a 256 x 256 pixel-registered dual-band FPA designed to operate simultaneously in the MWIR and LWIR spectral regions. We will also present imagery taken in the field of targets of military significance like armored vehicles, trucks, and helicopters. We have applied image fusion algorithms to the dual-band imagery. The results indicate that high-quality IR imagery can be obtained in both bands at operating temperatures lower than 65 K. We will then point out some of the shortcomings of this initial demonstration and recommend solutions.

---

[4] H. Pollehn and J. Ahearn, "Multi-Domain Smart Sensors," *Proceedings of the SPIE, Infrared Technology and Applications XXV,* Vol. 3698, Orlando, FL (1999).

[5] K. K. Choi, The Physics of Quantum Well Infrared Photodetectors, World Press, Singapore, (1997).

2.0 FPA FABRICATION

2.1 Detector Array

Details of the growth and processing of the dual-band QWIP FPAs used in this work have been published in Goldberg, et al.[6] Figure 1 shows the device structure schematically and Figure 2 is a scanning electron micrograph of several pixels of a dual-band QWIP FPA prior to indium bump deposition.

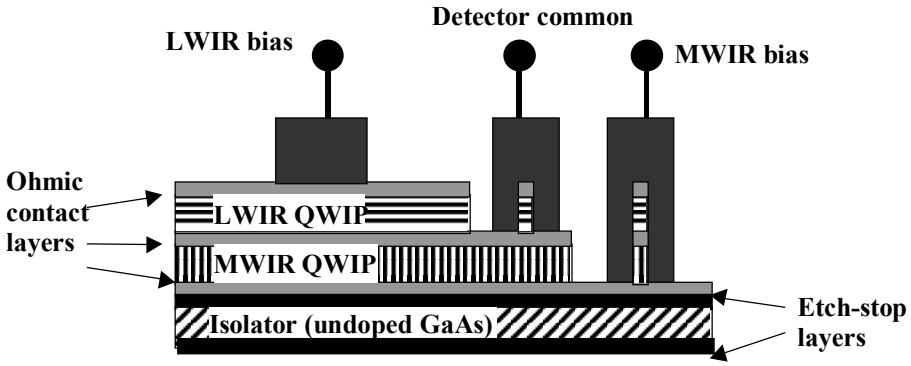

Figure 1. Schematic representation of the dual-band QWIP detector structure.

The pixels were square with a 40-μm pitch in both the x- and y-directions. The space between pixels was less than 2 μm leading to a fill factor of greater than 84% in the MWIR detectors (bottom layer) and greater than 77% for the LWIR detectors (top layer).

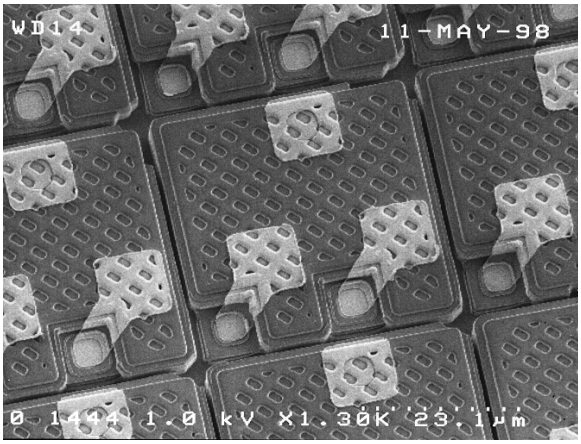

Figure 2. Section of two-color QWIP FPA prior to indium bump deposition, showing high optical fill factor, vertical sidewalls, and metal lines to each ohmic-contact layer.

---

[6] A. Goldberg, S. Wang, M. Sundaram, P. Uppal, M. Winn, G. Milne and M. Stevens, "Dual Band MWIR/LWIR Focal Plane Array Test Results," *Proceedings of the 1999 IRIS Detector Specialty Group Meeting on Detectors,* p. 87, ERIM (2000).

2.2 Read-out Integrated Circuit (ROIC)

Lockheed Martin Electronics and Missile Systems designed the ROIC. The simultaneously integrating and windowing ROIC was fabricated by using a 0.5-μm complementary metal oxide semiconductor (CMOS) process. It is designed to consume less than 50 mW power with a 5-V supply, uses a switched-capacitor frame snapshot architecture capable of frame rates up to 180 frames/s, and can provide variable bias for each color. The capacitance of the integration capacitor can be selected with a serial word command. In low-gain mode, the capacitance of the charge well is 1 pF, and in high-gain mode, the capacitance is 0.1 pF (well capacity 2.5×10^7 and 2.5×10^6 electrons, respectively for VDD = 5 V). This ROIC has also been used for dual-band LWIR/LWIR and MWIR/MWIR imaging FPAs.[7] In the high gain mode, a switched-capacitor filter, used to reduce output noise, is enabled. The implementation of this filter has been shown to reduce the FPA's ability to respond to transient signals.[8]

The ROIC provides bias to the detectors in the following way: The ohmic-contact layer between the MWIR and LWIR QWIP structures is made common for all pixels. This detector-common (DETCOM) voltage is then held above the main power bias for the ROIC chip (VDD). Bias levels on the LWIR and MWIR sections are maintained using separate bias supplies connected to the top and bottom ohmic-contact bumps of the detector pixels, respectively. The detector bias voltages need to be less than VDD. In this way, the LWIR structure is biased such that the electrons flow toward the substrate, and in the MWIR portion of the detector, the electrons flow away from the substrate.

3.0 RESULTS AND DISCUSSION

3.1 Laboratory Test Results

The tests on the dual-band FPA were done at ARL with the FPA installed in a liquid helium flow-through cryostat (Lakeshore MTD-150). The input clock and bias signals, as well as the output pixel data, were provided and collected by a configurable FPA drive electronics unit made by SE-IR Corporation. The pixel signals were digitized using 12-bit analog-to-digital converters (A/DC) capable of data rates up to 12 megapixels/s. The cryostat was equipped with an internal, cooled aperture wheel allowing for operation of the FPA under a wide range of background flux conditions (including zero-background).

Table 1 shows the bias values used to run the FPA. The frame rate used for tests was typically 60 Hz when viewing the blackbody source. This allowed for integration times as short as 80 μs and as long as 16 ms. For the dark-current tests, frame rates as low as 1 Hz and integration times as long as 800 ms were used.

Under typical tactical background conditions (background temperature ~300 K, f/2.0 to f/3.0) the photon flux in the MWIR portion of the spectrum covered by this FPA is approximately 10^9 photons/cm^2/s while that for the LWIR band is about one order of magnitude higher. Therefore, the MWIR portion of the array was nearly always run in the "high-gain" mode with charge well capacitance of 0.1 pF while the LWIR portion was run in "low-gain" mode with its charge well capacitance being 1.0 pF.

---

[7] G. Milne, K. Reiff, M. West, R. Martin, T. Faska, M. Sundaram, M. Taylor, R. Williams, and D. Hayden, "Advances in QWIP FPA (2-Color and 1-Color) Technology," *Proceedings of the 1999 Meeting of the IRIS Specialty Group on Passive Sensors,* ERIM (1999).

[8] J. Hubbs, D. Arrington, M. Gramer, and G. Doyle, "Radiometric Characterization of a Two Color Long/Long Wavelength, QWIP Focal Plane Array Under Low Background Conditions," *Proceedings of the1999 Meeting of the MSS Specialty Group on Infrared Detectors,* p. 105, ERIM (2000).

Table 1. Bias functions applied to the dual-band FPA and their values.

Bias name	**Function**	**Values used (V)**
VDD	Main power voltage for the ROIC.	5.00
DETCOM	Detector common voltage applied to the intermediate ohmic-contact layer.	5.50–6.50
DIBIAS1	Provide bias to the "top" ohmic-contact layer. Used to bias the LWIR device.	3.40–4.40
DIBIAS2	Provide bias to the "bottom" ohmic-contact layer. Used to bias the MWIR device.	2.00–3.00

The bias actually applied to the MWIR and LWIR sections of the detector array depends on all the values in

Table 1. For the LWIR detector, the bias is given by

$$LWBias = (DETCOM - VDD) + (3.90 - DIBIAS1) \text{ volts} \qquad (1)$$

and the bias on the MWIR detector is

$$MWBias = (DETCOM - VDD) + (3.90 - DIBIAS2) \text{ volts.} \qquad (2)$$

3.1.1 Spectral Response

The spectral response of the FPA was measured by forming an image of the output slit of a grating monochrometer and recording the changes in the outputs of the pixels as a function of wavelength. Figure 3 shows the results of these measurements. The response spectra measured for the two outputs of the FPA are slightly different from those reported in figure 3 of our previous work.[6] The earlier data were measured on single-pixel devices showed the peak of the MWIR response to be 5.1 μm with cut-on and cut-off wavelengths of 4.7 μm and 5.4 μm, respectively.

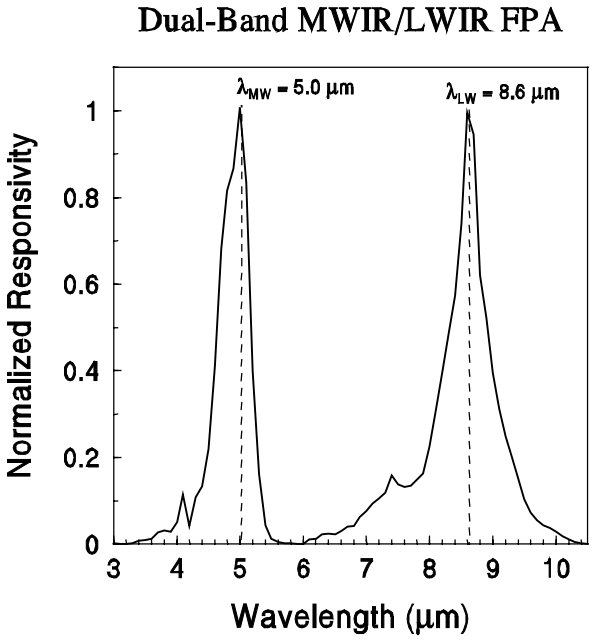

Figure 3. Normalized response spectra for the MWIR and LWIR sections of the dual-band QWIP FPA.

3.1.2 Dark Current and BLIP Temperature

For dark-current measurements, we placed the zero field-of-view cold stop in front of the FPA. The current was measured by integrating charge from the detectors for as long a time as necessary to fill the integration capacitor approximately halfway to saturation. A number of frames (typically 50) were then collected and averaged. The current was then calculated using

$$I = \frac{1}{\tau} N C_i G_{AD} \tag{3}$$

where N is the number of counts in the A/D (from 0 to 4095), C_i is the capacitance of the integration capacitor, G_{AD} is the gain of the A/D (V/count), and τ is the integration time. Similar data were collected with the shutter open (f/2.5 aperture) to measure the sum of the dark current and photocurrent. Figure 4 shows the results of these measurements. If we define the background-limited performance (or BLIP) temperature as the operating temperature at which the dark current and the background-induced photocurrent are equal, then the LWIR array is background limited below approximately 65 K and the MWIR array is background limited below approximately 95 K. The data agree well with the values predicted from tests performed on single-pixel detectors.

The dark-current data follow the expected exponential dependence on temperature with thermal activation energies of 226 meV for the MWIR structure and 120 meV for the LWIR part of the array. These energies correspond to wavelengths of 5.48 μm and 10.32 μm for the MWIR and LWIR structures, respectively. Figures 5 and 6 show the histogram and spatial distributions of the thermal activation energies for the LWIR and MWIR portions of the FPA. The mean activation energies were 119.3±3.0 meV and 226.3±9.97 meV, corresponding to nonuniformities in activation energy of 2.5% and 4.4% for the LWIR and MWIR arrays, respectively. However, since the dark current depends exponentially on the activation energy, these small variations in activation energy caused the dark current to vary by more than a factor of two across the FPA. The nonuniformity of the activation energy (and therefore, the dark current) is a major limiting factor in operating the QWIP FPA in the dark-current limit. At temperatures

above the BLIP temperature, the large variation in dark current limits the gain that can be applied to the output signals to a low value. Under these conditions, the span of output values covers the entire range of the A/DC.

To operate effectively at high temperatures, the variation in dark current should be no more than that of the photocurrent (5 percent or less). For a small change in activation energy δE_a, the corresponding change in dark current is $\delta I_d / I_d = -\delta E_a / kT$, where T is the operating temperature. To achieve a dark-current uniformity of 95 percent or better at 77 K, the activation energy must vary by no more than 0.33 meV or 0.275 percent. The observed variation in activation energy is an order of magnitude above this level.

The images in Figures 5 and 6 show that the activation energy decreases monotonically from left to right across the FPA for both the LWIR and MWIR arrays. This behavior is most likely indicative of variations in the material growth parameters (growth rates and/or alloy composition) across the chip. A substantial reduction in such nonuniformities is one factor that may allow for operation of QWIPs at higher temperatures.

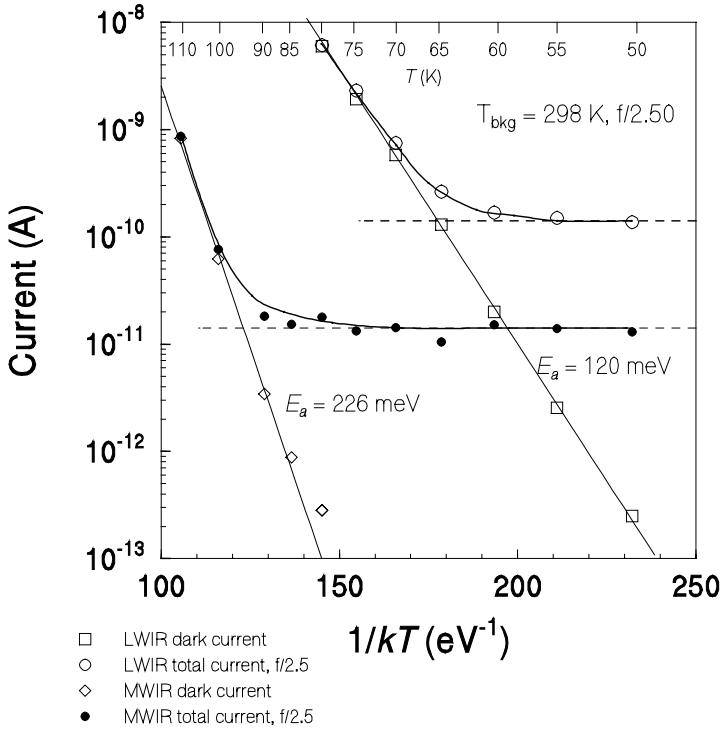

Figure 4. Mean dark current and total current for the MWIR and LWIR portions of the dual-band FPA. The background temperature was 298 K (25° C). The bias levels were 1.0 V for the LWIR and 2.0 V for the MWIR.

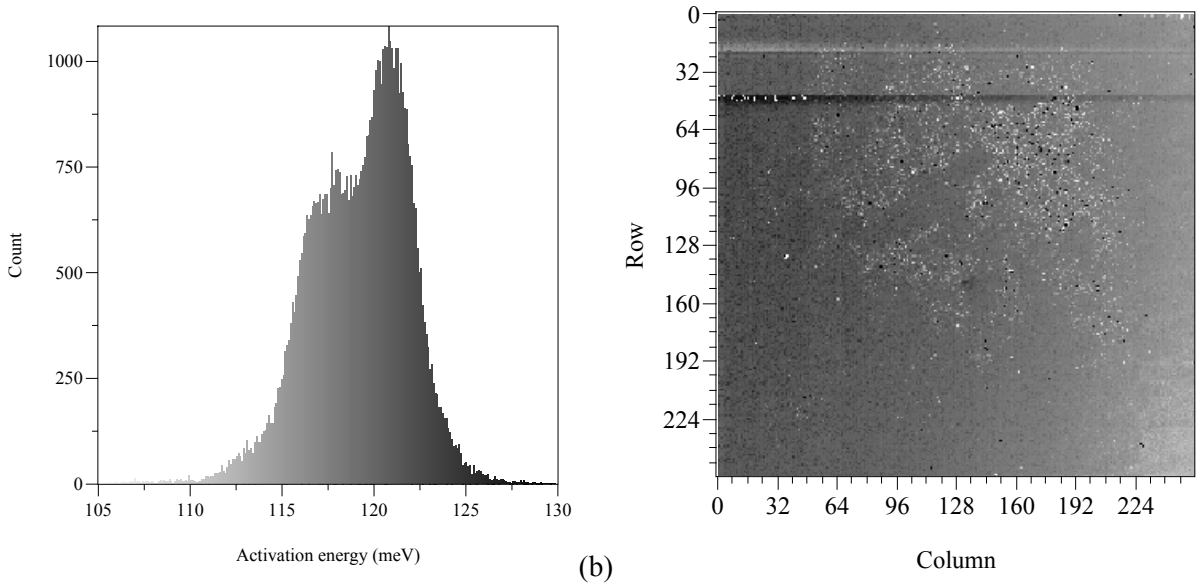

Figure 5. Histogram (a) and image (b) of the distribution of thermal activation energies for the LWIR pixels of the dual-band FPA. The mean activation energy is 119.3±3.0 meV.

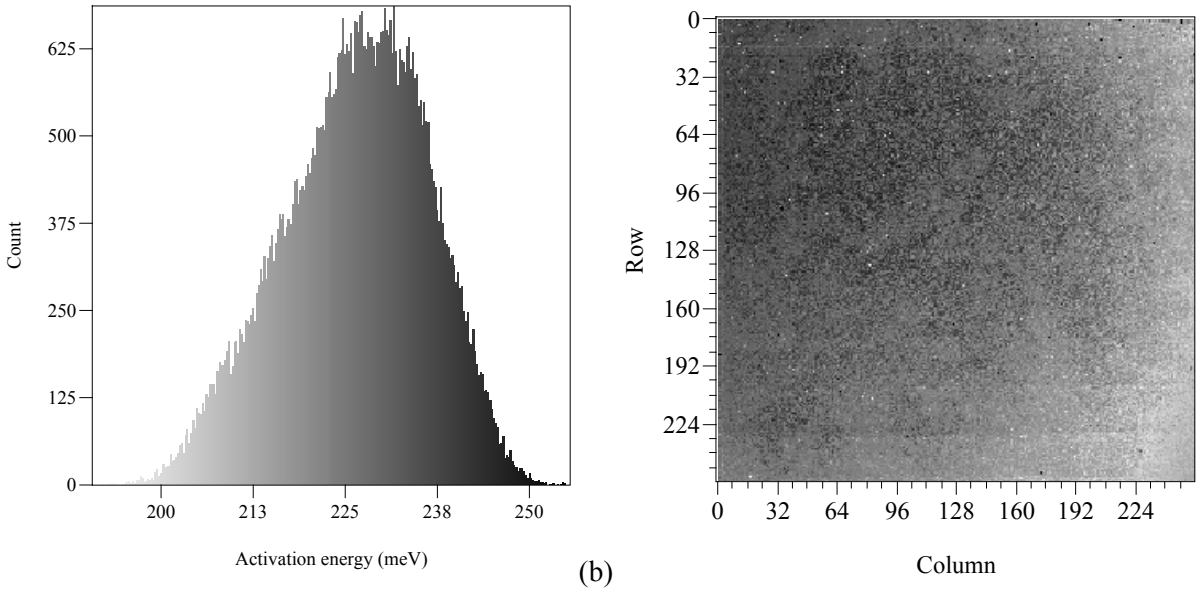

Figure 6. Histogram (a) and image (b) of the distribution of thermal activation energies for the MWIR pixels of the dual-band FPA. The mean activation energy is 226.3±9.97 meV.

3.1.3 Imaging Performance, Operability, and Uniformity

The noise equivalent temperature difference (NEΔT) was calculated from uncorrected imagery of an extended-area blackbody at different temperatures. The raw data consisted of many (usually 64) consecutive frames collected into a single file with a framegrabber built into the PC that operates the IR cam-

era electronics. The data were then analyzed using the NVESD 3-D noise model[9] to obtain the various components of NEΔT. The data was taken at blackbody temperatures covering a 12°C range in temperature from 20°C to 32°C; the calibration temperatures were defined as 22°C and 30°C. The data from each of the two bands was analyzed separately. Data were taken under a wide variety of operating conditions (bias levels) and at device temperatures ranging from 50 to 110 K.

We found that, under BLIP conditions, we could make the FPA performance relatively independent of the bias on the detectors by shortening or lengthening the integration time as needed to get the signals to cover most of the A/D range for a reasonable change in background temperature (~10 °C). Above the BLIP temperature, the large variation in output current made it difficult to find good operating conditions. In particular, in the temperature range between 65 and 70 K, the short integration times mandated by the relatively high dark currents in the LWIR part of the FPA also degraded the performance of the MWIR portion of the device. At temperatures of 70 K and above, it was impossible to operate the LWIR array and so the operating conditions were optimized for best MWIR performance.

Figure 7 shows the 3-D noise components of NEΔT for the LWIR (a) and MWIR (b) portions of the FPA at an operating temperature of 60 K. The integration time used was 8.0 ms, the LWIR bias was 1.0 V, and the MWIR bias was 2.0 V. The temporal NEΔT (N_{tvh}) was found to be approximately the same in both bands at about 32 mK. For the operating conditions described above, Figure 8 shows the histogram and image of the conversion efficiency of the LWIR array and Figure 9 shows those for the MWIR array. The imaging performance properties are summarized in Table 2 below.

Table 2. Performance properties of the dual-band MWIR/LWIR FPA at T=60 K.

Band	**Bias (V)**	**Mean Temporal NEΔT (mK)**	**Mean Conversion Efficiency (%)**	**Pixels with Response Outside ±10% of Mean**	**Pixels with Response Outside ±20% of Mean**
LWIR	1.00	34	2.61±0.119 (±4.56%)	229 (0.35%)	121 (0.18%)
MWIR	2.00	30	1.91±0.130 (±6.82%)	6346 (9.7%)	170 (0.26%)

The magnitude of the conversion efficiency as well as the pixel-to-pixel uniformity of the response are significantly better in the LWIR than in the MWIR. In both bands, the operability of the array is excellent with greater than 99.7 percent of the pixels having conversion efficiency values within 20 percent of the mean. The fixed-pattern noise is, as expressed by the value of N_{vh} in the 3-D noise, is significantly larger in the MWIR data as opposed to that for the LWIR array. This is probably due to the higher nonuniformity of response in the MWIR array relative to that of the LWIR array.

[9] J. D'Augustino and C. Webb, "3-D Analysis Framework and Measurement Methodology for Imaging System Noise," in *Infrared Imaging Systems: Design, Analysis, Modeling and Testing II*, G. Holst, Editor, *Proceedings of the SPIE* **1488**, 110-121 (1991).

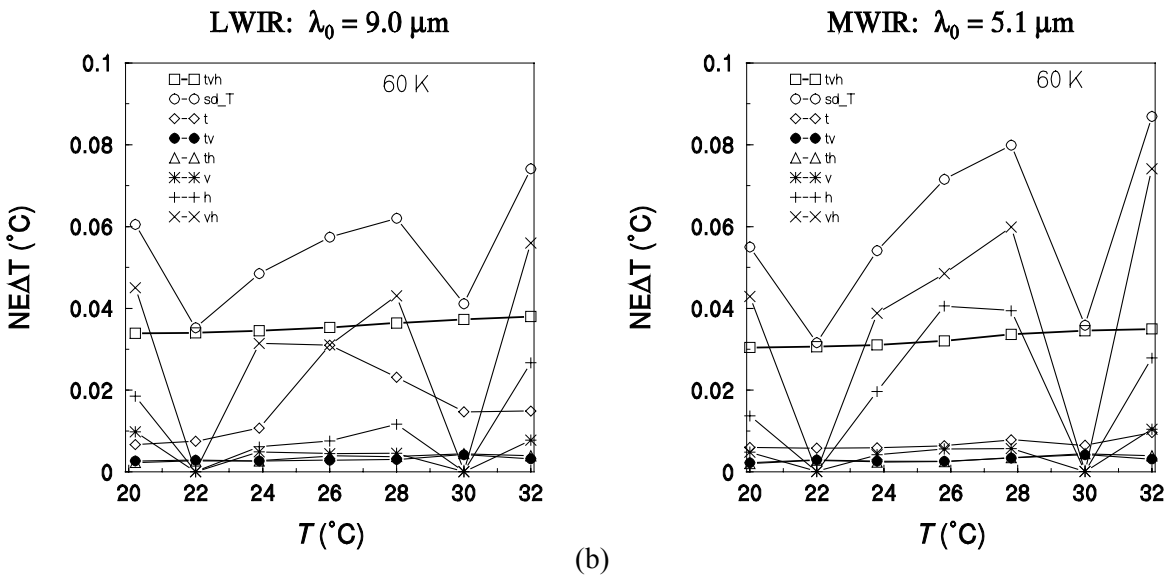

(a) (b)

Figure 7. 3-D noise components as a function of background temperature for the LWIR array (a), and the MWIR array (b) at a device temperature of 60 K. The integration time used was 8.0 msec, the LWIR bias was 1.0 V, and LWIR bias was 2.0 V.

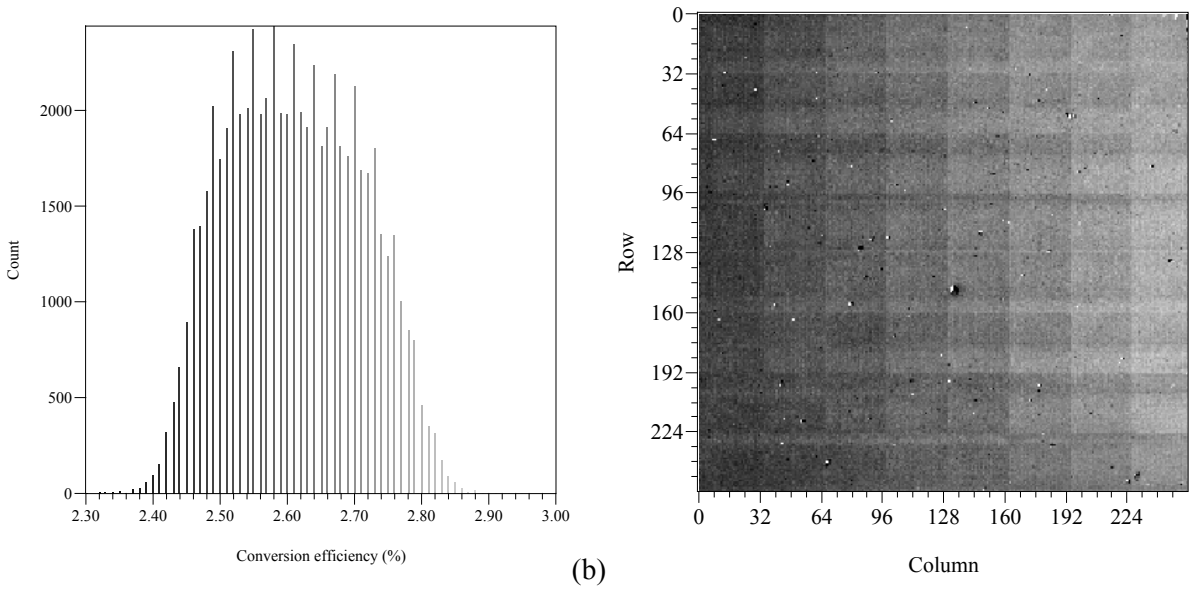

(a) (b)

Figure 8. Histogram (a) and grayscale image (b) of the conversion efficiency (quantum efficiency-gain product) for the LWIR part of the FPA.

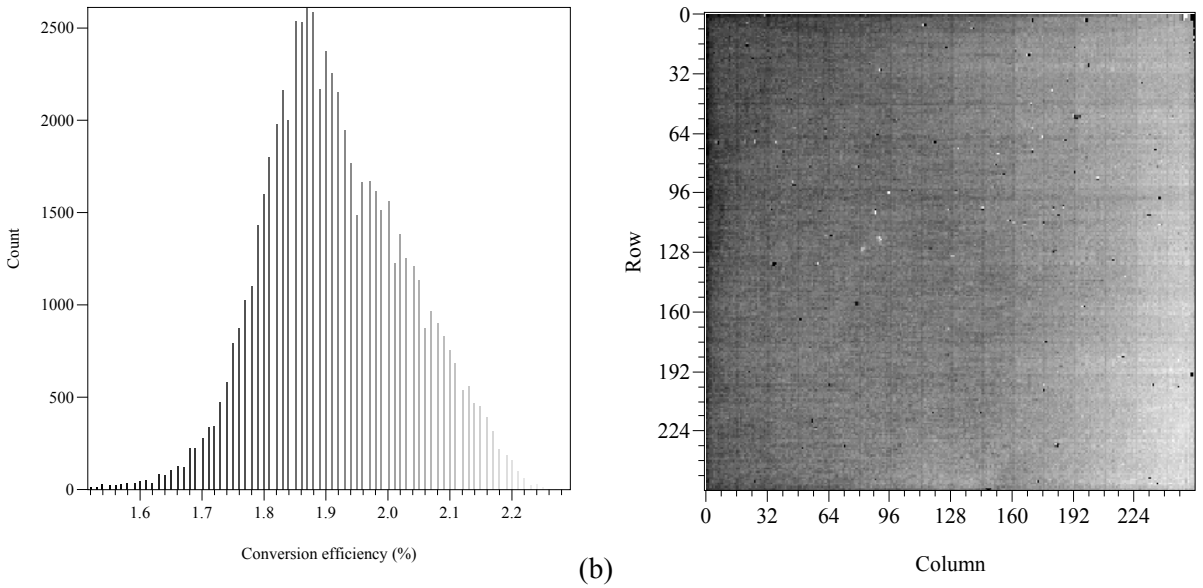

Figure 9. Histogram (a) and grayscale image (b) of the conversion efficiency (quantum efficiency-gain product) for the MWIR part of the FPA.

Figure 10 shows the results of measurements of temporal NEΔT as a function of operating temperature. Below 65 K, the arrays from both bands had similar values of NEΔT (between 30 and 40 mK). However, once the device temperature was higher than the BLIP temperature, the NEΔT rose dramatically in both bands. The NEΔT performance of the MWIR array degraded because short integration times were needed to keep the LWIR portion of the FPA from saturation (it was not possible to control the integration times for each band independently). At temperatures above 70 K, the operating conditions were optimized for the MWIR band. The NEΔT was approximately 30 mK for temperatures less than 90 K; at temperatures above 90 K, the dark current becomes dominant in the MWIR device, thus causing the NEΔT to rise sharply.

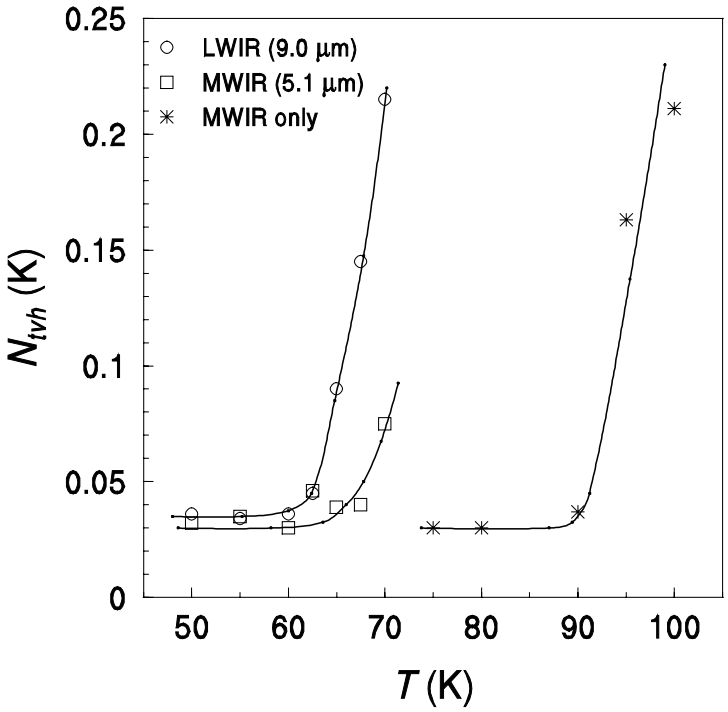

Figure 10. Mean temporal NEΔT (N_{tvh}) as a function of operating temperature for the dual-band FPA. The circles and squares are the values of NEΔT measured when operating conditions were optimized for running both bands simultaneously, the stars show the values of NEΔT measured when the conditions were optimized for the MWIR array alone. The lines are simply guides to the eye.

3.2 Image Fusion

The images acquired in the field tests performed with the dual-band QWIP FPA were subjected to a color fusion algorithm, developed at the Naval Research Laboratory [10] (NRL), in which pixel values from the LWIR and MWIR bands are assigned to color opponents such as red-cyan, blue-yellow, or green-magenta. Figure 11 illustrates this color fusion scheme using the red-cyan color opponents. Each pixel in the LWIR image is assigned a red value and each pixel in the MWIR image is assigned a cyan value (i.e., equal values of blue and green). For eight-bit color, the pixel values range from 0 to 255. Objects in the image with high brightness values in both bands will appear white; those with low brightness values in both bands will appear black. Objects with a high pixel value in the LWIR band and a low value in the MWIR band will appear red, and objects with a low pixel value in the LWIR band and a high pixel value in the MWIR band will appear cyan.

---

[10] D. Scribner, J. Schuler, P. Warren, M. Satyshur, M. Kruer, "Infrared Color Vision: Separating Objects from Backgrounds", *Proceedings of the SPIE - Infrared Detectors and Focal Plane Arrays* V, Vol. **3379**, (1998).

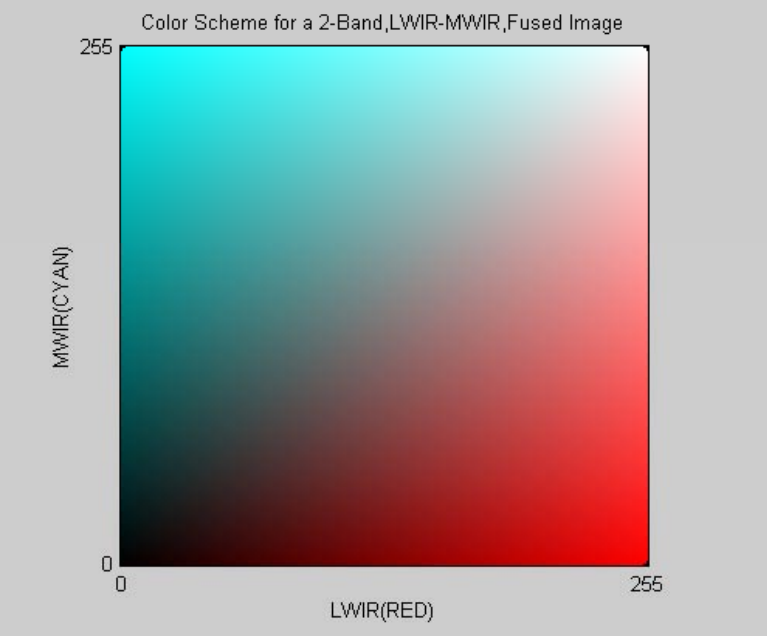

Figure 11. Red-cyan color scheme for fusing MWIR and LWIR images. The MWIR image is mapped to shades of cyan and the LWIR image is mapped to shades of red. Pixels with approximately equal values in the MWIR and LWIR will lie along the diagonal of the color diagram and will be represented by shades of gray.

In this scheme, bands in which the background and targets are highly correlated will yield fused images with little color contrast (the pixel data will lie roughly along the diagonal, [0,0] to [255,255], of the plot and the image will appear as shades of gray). Bands in which they are weakly correlated will yield maximum color contrast (the pixel data will be spread out in a direction orthogonal to the diagonal). Where the background is highly correlated and the target is only slightly different, the color contrast can be enhanced by performing a principal component (PC) transformation, normalizing the data along the PC directions (thereby stretching the data to fill the available color space), then performing the inverse transform back to the original color-opponent space.

3.3 Field Imaging Results

The dual-band FPA was installed in a portable camera system and taken to the field to image targets of military significance. Tests were conducted at Ft. A. P. Hill and at the Aberdeen Proving Ground (APG) during 1999. In both of these tests the imaging optical system was a 100-mm focal length f/3.0 dual-band lens made by Diversified Optical Products, Inc. With this lens, the instantaneous field of view (IFOV) was 0.4 mrad and the total FOV was 5.86° in both altitude and azimuth. Given the relatively short focal length of the optics (and therefore large FOV) it was difficult to resolve targets at ranges longer than 1 km. Nevertheless, it is possible to see the potential advantages of dual-band imaging with the images presented below. In addition, the placement of the MWIR spectral peak at 5.0 μm causes the FPA's response spectrum to miss much of the MWIR transmission window. This caused the MWIR imagery to be of lower contrast than that of the LWIR under all ambient conditions observed in these field tests. In addition, the relatively low conversion efficiency of the detectors necessitated the use of an integration time of approximately 10 ms.

3.3.1 Armored Vehicles

Figure 12 shows an M60 tank moving along a dirt and gravel road. The exhaust plume is more prominent in the MWIR image than in the LWIR image. In addition, the concrete slab in the foreground is very bright in the MWIR image, but relatively dark in the LWIR image.

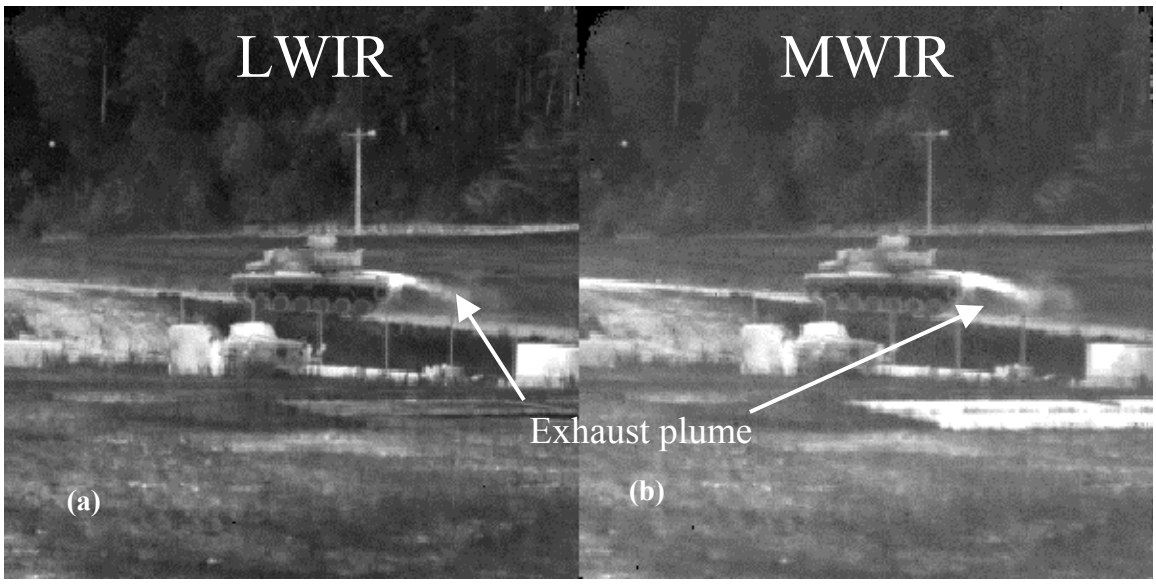

Figure 12. Image of an M60 tank taken with the dual-band MWIR/LWIR QWIP. The left-hand image (a) is the LWIR and the right image (b) is MWIR. Note that the exhaust plume of the tank and concrete slab are more prominent in the MWIR image.

Figure 13 shows an M60 tank and an M2 Bradley fighting vehicle at a range of approximately 200 m. This image was taken just before noon on a summer day. The M60 has kicked up a large dust trail that shows prominently in the LWIR image, as seen in Figure 13(a), but much less so in the MWIR image shown in Figure 12(b). Figure 13(c) shows the simple difference image of the two single-color images.

It is interesting to note that in image data collected during the MDSS field test in 1998 (in which separate MWIR and LWIR cameras were boresighted to give a simulated dual-band FLIR output) the dust plume from a moving vehicle appeared more prominent in the MWIR than the LWIR. This result has been reported elsewhere.[11] The results of an application of the color fusion algorithm described above of the MWIR and LWIR image data from Figure 13 and from the separate-camera image data are shown in Figures 14 (a) and (b), respectively. The data that were used to generate the images in Figure 14 were acquired at the same test range at the same season (late July), at approximately the same time of day (early afternoon) and under very similar meteorological conditions.

---

[11] A. Goldberg, T. Fischer, S. Kennerly, C. Garvin, M. Falco, and D. Campagna, *Proceedings of the 1999 Workshop on Hyperspectral/Multispectral Sensors: Measurements, Modeling and Simulation*, Huntsville, AL (to be published).

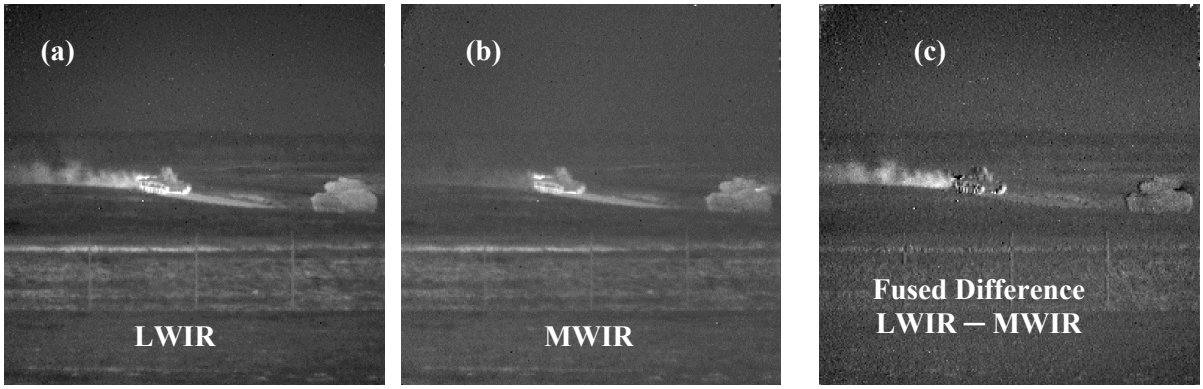

Figure 13. Simultaneous dual-band image of an M60 tank and an M2 Bradley fighting vehicle. The LWIR image (a) clearly shows a dust plume behind the tank that is barely visible in the MWIR image (b). In the MWIR image, the engine exhaust of the M2 can be seen more clearly than in the LWIR image. The fused difference image (LWIR – MWIR) is shown in (c); objects with large LWIR signatures (relative to MWIR) are bright and those with large MWIR signatures are dark.

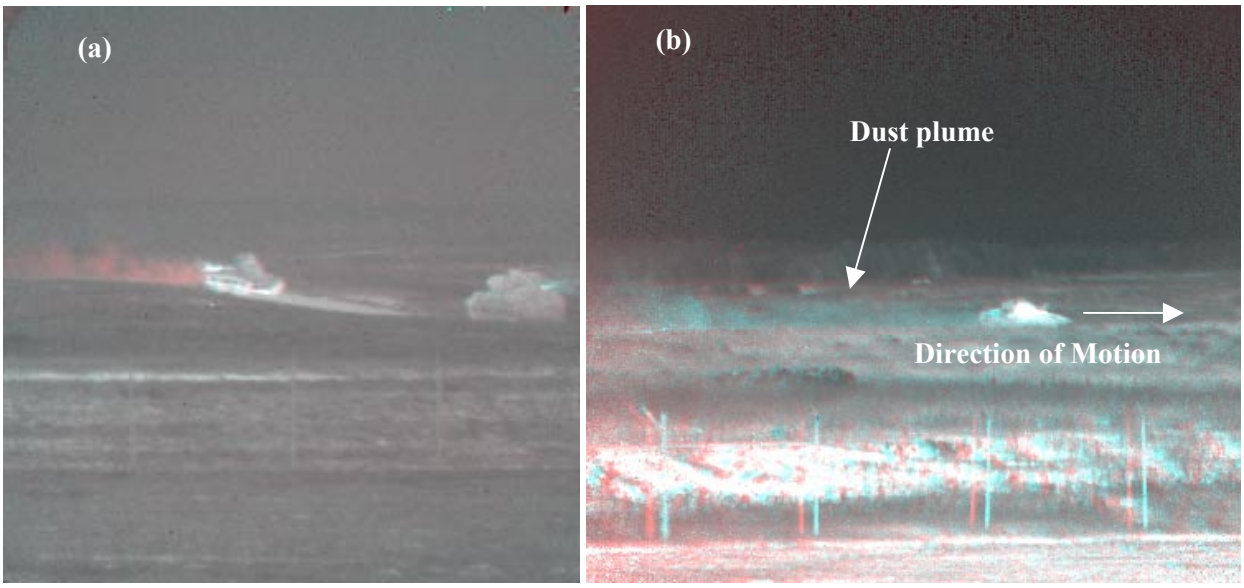

Figure 14. (a) Color fusion image of the LWIR and MWIR images shown in Figure 13. The dust plume from the M60 is most prominent in the LWIR data and therefore show appears red in the fused image. Conversely, the exhaust plumes from the vehicles emit strongly in the MWIR band and are therefore shown here as blue. (b) Color image fusion of MWIR and LWIR data from separate cameras. This image was acquired as part of the MDSS field test in July, 1998. The dust plume created by the motion of the M2 was more prominent in the MWIR image and is therefore shown as cyan in this image.

Figure 15 shows a series of images of an M1A1 tank moving down a gravel road in early evening. The left image is LWIR, the center image is MWIR and on the right is the color fusion image. In the tank's wake, a blast of warm air that slightly heated the leaves on the trees at the side of the road. This heating shows up best in the LWIR image. Therefore, the fused-color image displays the heated leaves as shades of red. As the tank gets closer, it is easier to see the MWIR signature (shades of blue) of the engine exhaust.

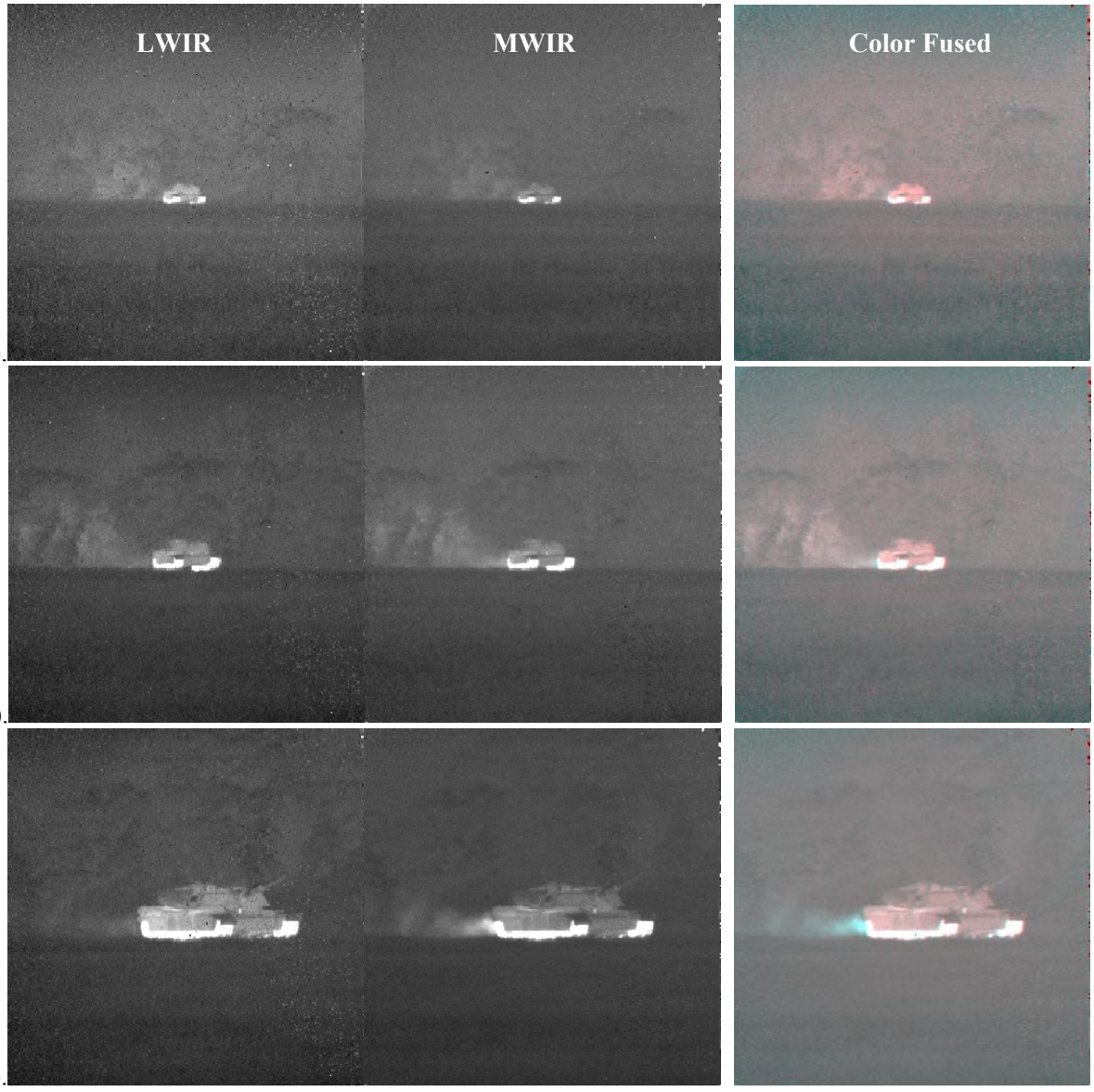

Figure 15. Images of an M1A1 tank approaching the camera. The bright areas behind the tank are tree leaves that were heated by the exhaust gases of the tank. The exhaust plume, which predominantly radiates in the MWIR, becomes prominent as the vehicle gets closer. The body of the tank itself appears to radiate most strongly in the LWIR and therefore appears red in the color fused images.

3.3.2 Trucks

Figure 16 is a dual-band image of a convoy of 3 military trucks moving down a gravel road at night; the range to the targets was approximately 500 m. The vehicles imaged were: a HMMWV, a Russian Zill-131 truck and an M35 truck. Figure 17 shows imagery of these targets at close range (approximately 100 m). The MWIR imagery of the Zill truck (Figure 17c) contains dark vertical lines extending from hot objects on the target. These artifacts do not appear in the LWIR image and are most likely caused by the switched-capacitor filter present in high-gain mode of the ROIC.

Figure 16. Dual-band image of three military trucks at a distance of approximately 500 m.

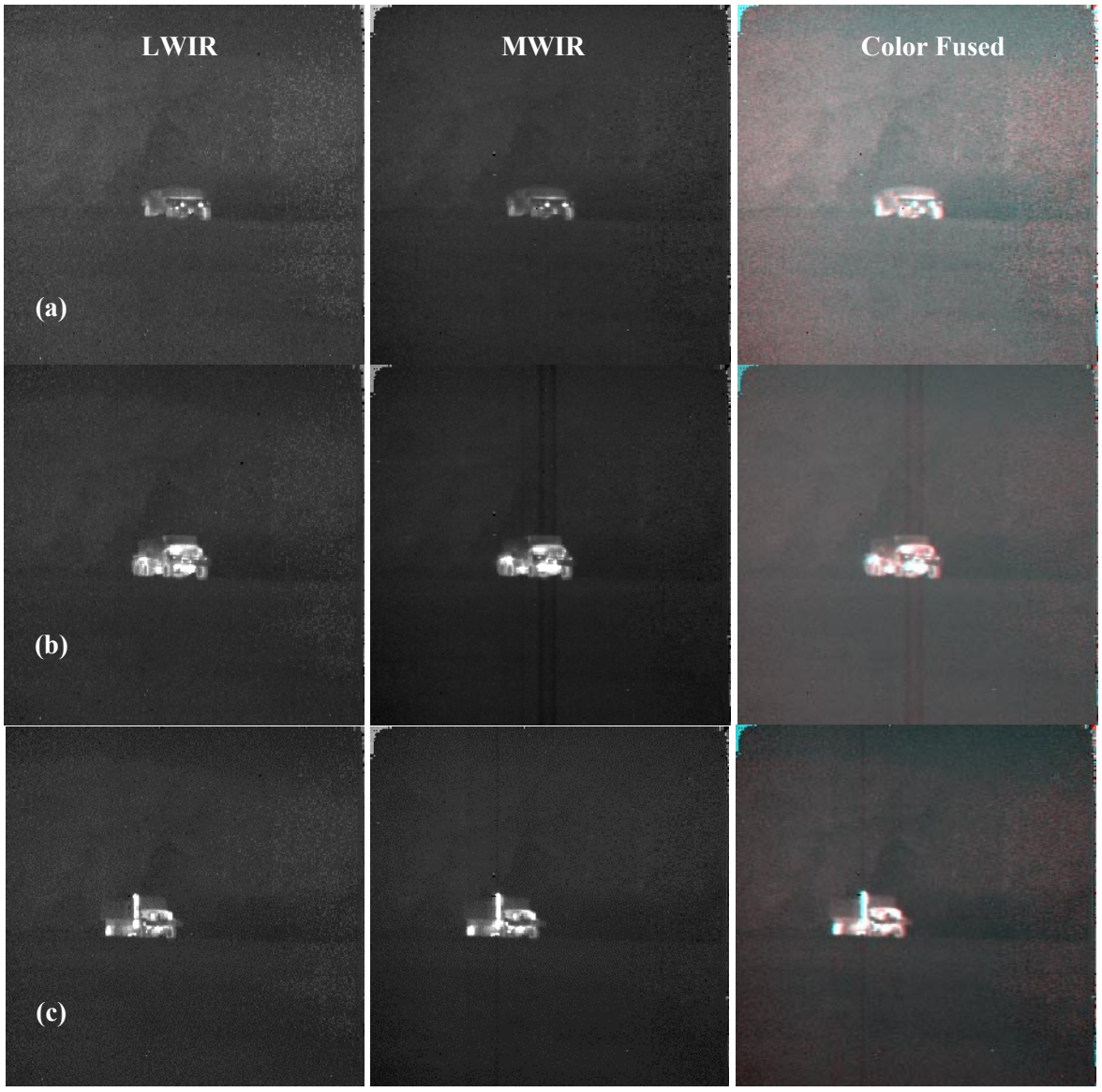

Figure 17. Dual-band images of a HMMWV (a), a Zill-131 (Russian) truck (b), and an M35 truck. The left hand images are LWIR, the center images are MWIR, and the right hand images are the results of color fusion.

3.3.3 Helicopters

Figure 18 shows dual-band images of different helicopters acquired at night at relatively close range (less than 500 m). The smearing of the signature of the rotor blades can be clearly seen in the MWIR image; it is not nearly as apparent in the LWIR image. In addition, the hot engines create dark vertical line artifacts in the MWIR image that are not seen in the LWIR image (not shown in the images in Figure 18). Both of these artifacts are caused by the switched-capacitor filter enabled for the MWIR portion of the FPA (due to the need to run at high gain).

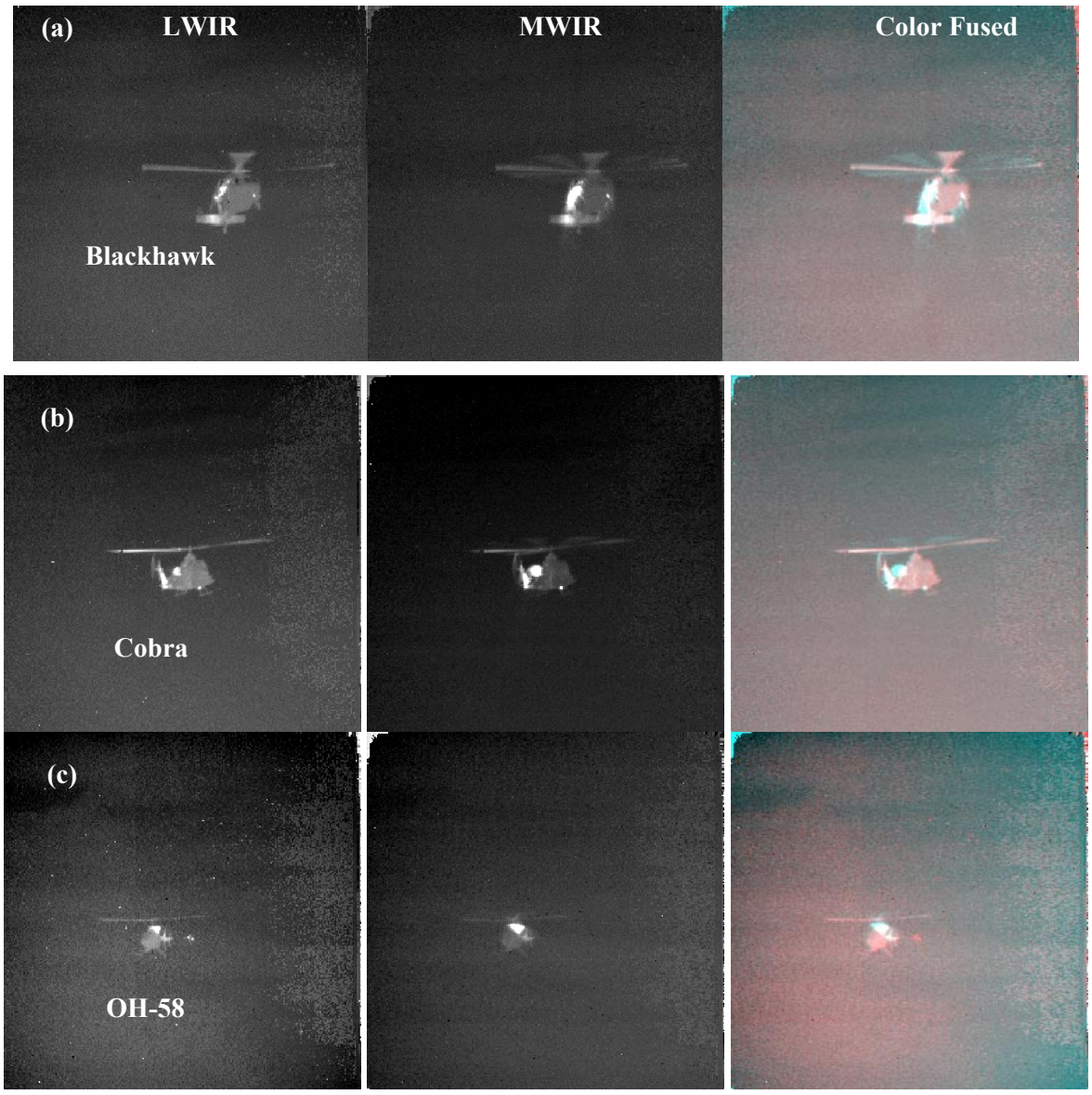

Figure 18. Dual-band images of three different helicopters: Blackhawk (a), Cobra (b), and OH-58 (c).

4.0 SUMMARY AND CONCLUSIONS

We have presented the results of laboratory and field tests of a pixel-registered, simultaneously integrating dual-band FPA operating in the MWIR (peaked at 5.0 μm) and in the LWIR (peaked at 8.6 μm) made using QWIP technology. The laboratory tests indicated that the array had excellent operability

(>99.7 percent) and good imaging performance in both bands for temperatures less than 65 K. The temporal NEΔT was found to be approximately 32 mK in both bands below 65 K and approximately 30 mK for the MWIR band for temperatures less than 90 K. The field performance of the dual-band QWIP FPA was very good, given the parameters of the optical system. Specific issues in the level of performance (i.e., conversion efficiency, spectral placement) of the individual pixels need to be addressed. However, the operability and uniformity of the FPA in both bands is quite impressive. Single-pixel results on dual-band QWIP material lattice-matched to an InP substrate that was grown at ARL indicate that these issues are not insurmountable.[12] Dual-band QWIP FPAs with considerably higher conversion efficiencies than those quoted here in both the MWIR and LWIR bands are possible. The smearing of imagery of fast-moving targets in the MWIR is a direct result of a sub-optimal implementation of a switched-capacitor filter in the high-gain mode of the ROIC. Others have observed a behavior very much like dielectric relaxation in QWIPs at low temperatures and backgrounds. We believe that under the conditions in which this FPA was operated, the dielectric relaxation would have affected the MWIR imagery much less than what we observed. A minor modification to the ROIC would almost completely eliminate the observed image smearing. If the MWIR conversion efficiency was 10% (as opposed to the measured 2%), the additional photocurrent would short out any residual dielectric relaxation effects, thus allowing for sharp MWIR images. We expect to take delivery of an improved dual-band QWIP FPA later this year.

It appears from the field imagery that the differences in the MWIR and LWIR signatures of the targets studied were not nearly as significant as those of the disturbances that the targets made to their immediate environment. This would include the exhaust plumes from engines, dust kicked up from the ground, and heat transferred from the targets to their surroundings. However, even images taken under similar conditions can yield vastly different results. The two images shown in Figure 14 were both taken in mid-summer at the same test site at nearly the same time of day and under very similar meteorological conditions. However, in Figure 14 the dust kicked up by the moving vehicle emits and/or reflects more LWIR light than MWIR, while in Figure 15, the dust emitted/reflected more MWIR than LWIR light. Evidently, subtle differences in the conditions can have a major impact on the observed imagery.

One of the principal motivations behind dual-band IR imaging systems has been the supposed ability to pick out targets in a cluttered environment better than a single-color system or similar performance. In our field tests reported here, none of the targets were embedded in any sort of a cluttered setting. Therefore, we find it difficult to conclude from these data whether this MWIR/LWIR dual-band camera will be able to fulfill the promise of enhanced target detection/recognition performance in such situations. However, in a previous field test using separate MWIR and LWIR cameras, the ATR performance was enhanced significantly when imagery from both cameras was used over that for single color data.[13]

ACKNOWLEDGEMENTS

We are grateful for the assistance of H. Pollehn and J. Ahearn for management of the MDSS Federated Laboratory program. We would like to thank John Hopkins of ARL for assistance in arranging the field test at the Aberdeen Proving Ground and Glen Horan of NVESD for assistance with the field test at Ft. A. P. Hill. We would also like to thank Charles Garvin, formerly of Sanders, A Lockheed Martin

---

[12] J. Little, S. Kennerly, R. Leavitt, M. Lucas, and K. Olver, "A New Two Color Infrared Photodetector Design Using InGaAs/InAlAs Couple Quantum Wells," *Proceedings of the 1999 Meeting of the MSS Specialty Group on Infrared Detectors,* p. 127, ERIM (2000).

[13] S. Der and N. Nasrabadi, "Analysis of Dualband Passive Infrared Imagery for Automatic Target Detection," *Proceedings of the 1999 Workshop on Hyperspectral/Multispectral Sensors: Measurements, Modeling and Simulation*, Huntsville, AL (to be published).

Company for assistance in various field data collections. The ROIC used for this work was designed and fabricated under the Advanced Multiple Quantum Well Technology (AMQWT) program funded by the Air Force Research Lab, contract number F08630-96-C-0083, managed by Mr. David Hayden and Mr. John Winterberger. We would also like to acknowledge the support of Dr. Walt Dyer and LTC Buckley of the Ballistic Missile Defense Organization.